PHILOSOPHICAL TRANSACTIONS OF THE ROYAL SOCIETY A MATHEMATICAL, PHYSICAL & ENGINEERING SCIENCES

Changes in the potential distribution of humid tropical forests on a warmer planet

Przemyslaw Zelazowski, Yadvinder Malhi, Chris Huntingford, Stephen Sitch and Joshua B. Fisher

Phil. Trans. R. Soc. A 2011 **369**, 137-160
doi: 10.1098/rsta.2010.0238

PHILOSOPHICAL TRANSACTIONS OF THE ROYAL SOCIETY A

Phil. Trans. R. Soc. A (2011) **369**, 137–160
doi:10.1098/rsta.2010.0238

Changes in the potential distribution of humid tropical forests on a warmer planet

By Przemyslaw Zelazowski[1,*], Yadvinder Malhi[1], Chris Huntingford[2], Stephen Sitch[3] and Joshua B. Fisher[4]

[1]*Environmental Change Institute, School of Geography and the Environment, University of Oxford, Oxford OX1 3QY, UK*
[2]*Centre for Ecology and Hydrology, Wallingford OX10 8BB, UK*
[3]*School of Geography, University of Leeds, Leeds LS2 9JT, UK*
[4]*NASA Jet Propulsion Laboratory, California Institute of Technology, Pasadena, CA 91109, USA*

The future of tropical forests has become one of the iconic issues in climate-change science. A number of studies that have explored this subject have tended to focus on the output from one or a few climate models, which work at low spatial resolution, whereas society and conservation-relevant assessment of potential impacts requires a finer scale. This study focuses on the role of climate on the current and future distribution of humid tropical forests (HTFs). We first characterize their contemporary climatological niche using annual rainfall and maximum climatological water stress, which also adequately describe the current distribution of other biomes within the tropics. As a first-order approximation of the potential extent of HTFs in future climate regimes defined by global warming of 2°C and 4°C, we investigate changes in the niche through a combination of climate-change anomaly patterns and higher resolution (5 km) maps of current climatology. The climate anomalies are derived using data from 17 coupled Atmosphere–Ocean General Circulation Models (AOGCMs) used in the Fourth Assessment of the Intergovernmental Panel for Climate Change. Our results confirm some risk of forest retreat, especially in eastern Amazonia, Central America and parts of Africa, but also indicate a potential for expansion in other regions, for example around the Congo Basin. The finer spatial scale enabled the depiction of potential resilient and vulnerable zones with practically useful detail. We further refine these estimates by considering the impact of new environmental regimes on plant water demand using the UK Met Office land-surface scheme (of the HadCM3 AOGCM). The CO_2-related reduction in plant water demand lowers the risk of die-back and can lead to possible niche

*Author for correspondence (przemyslaw.zelazowski@ouce.ox.ac.uk).

Electronic supplementary material is available at http://dx.doi.org/10.1098/rspa.2010.0238 or via http://rspa.royalsocietypublishing.org.

One contribution of 13 to a Theme Issue ‘Four degrees and beyond: the potential for a global temperature increase of four degrees and its implications’.

expansion in many regions. The analysis presented here focuses primarily on hydrological determinants of HTF extent. We conclude by discussing the role of other factors, notably the physiological effects of higher temperature.

Keywords: tropical forests; climate change; climate patterns; water stress; maximum climatological water deficit; carbon dioxide

1. Introduction

Tropical forests cover 10 per cent of all land area ($1.8 \times 10^7\,km^2$; [1]), and represent about half of global species richness [2]. Clearing of these forests is estimated to account for 12 per cent of anthropogenic carbon emissions [3], which are partly offset by a forest carbon sink with enhanced forest productivity and biomass linked to elevated atmospheric CO_2 concentrations [4]. Over half of the tropical-forest area ($1.1 \times 10^7\,km^2$) is represented by humid tropical forests (also called 'moist tropical forests', 'wet tropical forests', or 'tropical rainforests'; hereafter abbreviated to HTFs), characterized by high tree-species diversity and high biomass density [5–7].

Tropical-forest boundaries are often delineated by overlaying land-cover maps with maps of ecological zones defined by climate (e.g. [8,9]), as climate generally exerts the largest influence on the distribution of vegetation types at the global scale [10]. However, there is no commonly accepted delineation of tropical-forest types because, in reality, the transition between them tends to be gradual. Ecological zones concerning tropical forests are usually based on precipitation, and sometimes also temperature and humidity patterns. This study critically examines a number of approaches to describe climatic conditions that are optimal for HTFs, before proceeding with the study of climate impacts on this biome's potential distribution.

Lewis [11] characterized HTFs as having high annual rainfall (>1500 mm) and low seasonality defined by less than six months of dry season with monthly precipitation greater than 100 mm $month^{-1}$. Malhi *et al.* [12] found the same value of annual rainfall (1500 mm) to be a reasonable threshold for viable broadleaf evergreen forests of Amazonia. A second boundary proposed in that study, related to the strength of the dry season, was the maximum climatological water deficit (MCWD; see §2) between −200 and −300 mm. The study, in some ways a precursor to the analysis presented here, used the key assumption that each month, the forest evapotranspires approximately 100 mm of water. Such an evapotranspiration rate for non-drought-stressed HTFs is widely used, and it reflects the findings from observational studies (e.g. Kumagai *et al.* [13]; Malhi *et al.* [14]), although recent estimates suggest that it may be somewhat higher [15].

Temperature may be used to refine the estimate of water stress; for example, Mayaux *et al.* [1] and Food and Agriculture Organization (FAO) [8] defined the HTF climatological niche as having a maximum of three dry months with monthly rainfall (in millimetres) lower than twice the mean temperature (in °C), although such an empirical combination of temperature and precipitation variables appears to have little mechanistic justification. Richards *et al.* [16] advised a broad classification of tropical climates in relation to vegetation based

on annual rainfall, temperature and the perhumidity index (PI [17]) that attempts to summarize both the dry- and wet-season precipitation characteristics into a single index value. In this scheme, a low-temperature boundary is used to separate a group of tropical climates associated with biologically distinct *montane* forests, for which humidity, sunshine and cloudiness also play a role in defining the boundaries.

Climate change will manifest itself by changes in temperature and precipitation (see Betts *et al.* [18] for relevant analysis), as well as other aspects of the climate system, including humidity, radiation and wind. All of these changes may, to a varying degree, have consequences for the future distribution of conditions favoured by HTFs. Related to this problem is the concern about climate-induced 'die-back', which first received attention following Cox *et al.* [19]. A simple examination of the climate-related changes in the HTF climatological niche (defined in the current climate) provides insight into the future extent of this biome. However, potential shifts in the environmental optima, or thresholds, of biomes also need to be considered. For example, plant water-use efficiency (the amount of carbon assimilated per unit of water transpired) increases with atmospheric CO_2 concentration. Increasing temperature may have a positive or negative impact on photosynthesis and net carbon uptake [4,20,21]. Very high temperatures may also cause the closure of stomata. Hence, the impact of new climate regimes on plant physiology may be a key to determine the future distribution of HTFs. Although the issue is complex [20], and not yet fully understood, the ongoing ecological response of HTFs to climate change informs the debate, and the role of increased CO_2 emerges as an important factor to be considered [4].

Research concerned with climate-change impacts on tropical forests has tended to focus on Amazonia and address the possibility of climate-induced die-back [12,22–25]. Owing to teleconnections with other components of the climate system, this region has been recognized as one of the Earth system's potential tipping elements [26]. In reality, factors other than climate may also contribute to the major loss of Amazonian HTFs, such as anthropogenic deforestation and interactions between deforestation and fire spread. Die-back may be exacerbated by the interaction between these factors and imposed climate change [27]. The majority of literature devoted to the risk of forest die-back across the tropics has attempted to address this problem with Dynamic Global Vegetation Models (DGVMs) driven by future projections of climate change. The results depended largely on the assumed future climate pathway, and on the individual DGVM selected [28,29]. For example, early studies were based on the UK Hadley Centre model HadCM3, which predicts very dry and hot conditions over Amazonia, enhanced by feedback from forest die-back [19,24,30]. In that framework, the rising temperatures caused a strong decline in net primary production [31], which led to the loss of forest cover, as explicitly simulated by the Top-down Representation of Interactive Foliage and Flora Including Dynamics (TRIFFID) DGVM [32,33]. Subsequent studies attempted to account for uncertainty in future climate through either the use of conditions predicted by one Atmosphere–Ocean General Circulation Model (AOGCM) with various alternative parametrizations [25], or a number of AOGCMs (e.g. [34–37]). None of these studies reported any potential for new areas to be colonized by HTFs. It is possible that the low spatial resolution of the frameworks used (minimum of 60 km in the study

by Cook & Vizy [38]) is inadequate to describe the broad distribution and variability of climatic factors and risks. Small-scale variation, notably linked to topography, may facilitate greater ecosystem resilience than what the models suggest [39,40].

In this study, we explore the possibility for retraction or expansion of HTFs under twenty-first century anthropogenic global warming. First, we take an empirical approach to defining the current climatological niche of HTFs. We then use projections from 17 coupled AOGCMs, downscaled using contemporary climatological data, to explore (i) the potential variation of this niche, assuming no impact of new climate regimes on plant water demand, and (ii) the consequences of potential change in plant water demand. Specifically, we ask the following questions:

— Which scalable climatological indices best define the current boundaries of the HTF biome, and what are the appropriate threshold values of these indices?
— What is the spatial pattern and magnitude of potential humid forest expansion and retraction considered over 17 different climate models?
— What does the consideration of higher resolution climatological patterns add to our understanding of potential risk regions and potential HTFs refugia that are resilient to climate change?
— How does the introduction of environmental controls on the plant physiology, which influence water demand, affect the likelihood and pattern of potential niche contraction or expansion?

The novel contributions in this work arise from a combination of (i) the empirical derivation of the hydrological threshold for tropical forests worldwide, (ii) consideration of multiple climate models, (iii) consideration of fine-scale variation in climate patterns, and (iv) inclusion of effects of new climate regimes on plant water-use efficiency. It is worth noting that this analysis focuses on ecosystem water demand and its potential variation, as inferred from the canopy conductance and photosynthesis model. It does not consider all ecophysiological influences of atmospheric change, for example high CO_2 altering the competitive balance between C3 photosynthesis-dominated forests and C4-dominated grasslands. Such ecophysiological considerations could be incorporated by employing a dynamic vegetation model, but are limited by a poor understanding of what the ecophysiological responses and thresholds are, and the extent to which plant processes can acclimate to higher temperatures. The merits and uncertainties of incorporating other ecophysiological processes are presented in §4.

2. Methods

(*a*) *Contemporary distribution of humid tropical forests and their niche*

Spatial distribution of tropical vegetation biomes was assessed based on the Global Land Cover 2000 dataset ([41]; figure 1) derived from satellite data. It employed the Land Cover Classification System of the FAO in which

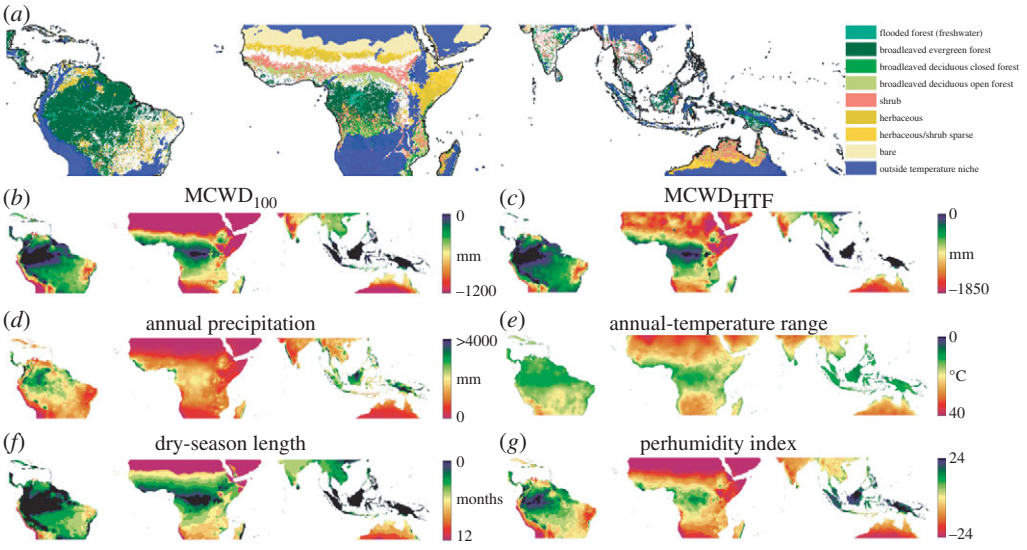

Figure 1. (*a*) Vegetation classes in the tropics. Areas too cold for lowland HTFs are shaded in blue. White areas within continents are covered by either anthropogenic or mixed land-cover types, and were not used in the analysis. (*b–g*) Key climate variables linked to the distribution of tropical biomes (see also table 1). Underlying data source: Global Land Cover 2000 and WorldClim datasets.

vegetation types are based on vegetation form (e.g. trees, shrubs), density, leaf type and phenology. HTFs were assumed to be represented by a class of evergreen broadleaved forests and forests flooded by freshwater, both within the tropics.

A number of variables related to surface precipitation and temperature were considered for the definition of climatological niche of the contemporary HTFs. The explanatory power of each variable in terms of the distribution of HTFs and other tropical vegetation types (non-evergreen forest types, dense non-forest vegetation and sparse non-forest vegetation) was assessed using multi-nomial logistic regression. Each variable's range, specific to a region within the tropics (Americas, Africa and south and insular Asia, referred to as 'Asia') was split into 44 equal bins (except for the dry-season length with only 12 bins), which were represented by a high number of vegetation-type counts (pixels). The assessment included three criteria: (i) deviance, which depicts the variable's overall capacity to predict the composition of vegetation types, (ii) the root mean-squared error (RMSE), calculated for HTFs, reflecting the difference between the predicted and actual contribution from HTFs across the variable's gradient, and (iii) the predictor's ability to capture both high and low probability of HTF occurrence, as inferred from the shape of the fitted curve. The considered climatic predictors included 19 variables of the Worldclim dataset [42], and 10 additional variables derived for this study, which included MCWD ([12]; equation (2.1)), PI [17], dry-season length (defined as in [1,8]; see §1), annual actual evapotranspiration (ET), and minimum and maximum mean monthly temperature (and the resulting annual-temperature range).

The MCWD was derived in four ways, all of which conformed to the following general definition:

$$\left.\begin{aligned} &\mathrm{CWD}_n = \mathrm{CWD}_{n-1} + P_n - \mathrm{ET}_n; \quad \mathrm{Max}(\mathrm{CWD}_n) = 0; \\ &\mathrm{CWD}_n = \mathrm{CWD}_{12}; \quad \mathrm{MCWD} = \mathrm{Min}(\mathrm{CWD}_1, \ldots, \mathrm{CWD}_{12}) \end{aligned}\right\}. \tag{2.1}$$

Hence, the MCWD is the most negative mean monthly value of climatological water deficit (CWD) across the annual cycle, with each monthly step inferred from the difference between precipitation P and evapotranspiration ET.

The definition of monthly evapotranspiration ET varied depending on the approach taken. First (MCWD_{100}), the monthly ET was assumed to be constant (as in [12]). The second approach ($\mathrm{MCWD}_{\mathrm{ET}}$) used mean monthly ET estimates based on data from Fisher *et al.* [43], with a spatial resolution of 0.5°. As this second approach takes vegetation indices as input variables, it predefines to some extent the HTF niche. To bypass this issue, the third approach ($\mathrm{MCWD}_{\mathrm{HTF}}$) aimed at assessing the magnitude of ET in the hypothetical scenario, in which the whole extra-tropics are potentially covered by HTFs. The ET over this region was calculated based on the median value of the vegetation seasonality and density (described by spectral vegetation indices) inside the areas currently covered by HTFs, and the corresponding atmospheric moisture (described by water-vapour pressure). The simulation preserved the original values of net radiation and maximum air temperature, which meant that the primary drivers of potential evapotranspiration were unaffected.

The PI [17], another considered metric related to plant water stress, measures the degree of continuity of wetness (or perhumidity) of monthly precipitation series in a tropical climate. Each month is assigned a score, depending on the amount of rainfall in both that and the previous month. The sum of scores reflects both the dry- and wet-season characteristics of the climate.

Subsequent analysis of the future extent of the HTF climatological niche was based on the variables that were found to be the best predictors of its contemporary distribution. In addition, the low-temperature boundary (mean annual temperature below 20°C, and a coldest monthly mean below 18°C) based on Richards [16] was used to separate lowland rainforests from montane forests and other cooler forest biomes.

(*b*) *Climate-change patterns*

Climate-change patterns (or 'pattern scaling'), as defined by Mitchell *et al.* [44] and Huntingford & Cox [45], are a method of providing monthly and regional estimates of variability in surface climate, and as a function of mean global warming. The underlying assumption is that attributes of surface climate vary approximately linearly with mean global warming over land, and the derived regression coefficients are referred to as 'patterns'. The initial application of this approach was to allow rapid interpolation from the existing global climate model simulations to surface climate conditions associated with new pathways in atmospheric greenhouse-gas concentrations. The radiative forcing associated with such concentrations is calculated and used to drive a simple global thermal model (also called the Simple Climate Model; Wigley *et al.* [46]), leading to predictions of mean warming over land required to multiply the patterns. Although pattern scaling is an effective, and policy-relevant, way of generalizing climate data,

it needs to be remembered that the patterns reflect only a portion of climate change which is scalable with warming over land or globe; thus they do not fully reflect the variability in scaled variables, including the highly variable precipitation [44,47].

This study focuses on climate regimes representing global warming of 2°C and 4°C (above pre-industrial levels; referred to as the '+2°C' and '+4°C' scenarios), simulated with coupled AOGCMs, which were employed in the Fourth Assessment (AR4) of the Intergovernmental Panel for Climate Change. Climate patterns were derived for 17 out of 24 AOGCMs (data available at the World Climate Research Programme's Coupled Model Intercomparison Project (WCRP CMIP3) portal; https://esg.llnl.gov:8443). The other seven AOGCM datasets were excluded as they lacked some of the required data. Key variables that were scaled for each AOGCM, and all of which are important to land-surface functioning, included: temperature, relative humidity, precipitation and radiation. The use of pattern scaling allowed emulation of the '+4°C' scenario, even if it was not present in the AOGCM data.

Spatial resolution of climate data varies between AOGCMs, although it is generally of the order of hundreds of kilometres. For this analysis, resolutions were homogenized as follows. First, all data were interpolated to a resolution of 1° with the Climate Data Operators package (www.mpimet.mpg.de/~cdo/). Subsequently, the data were re-mapped onto the HadCM3 model grid. The mapping procedure distinguished between land, ocean and mixed areas, and allowed for minor spatial shifts in grid boxes in order to preserve the land/ocean contrast in surface variables.

In order to circumvent the problem of known biases in the description of the current climate by some AOGCMs, which is especially important in the case of tropical rainfall, each AOGCM precipitation pattern (ΔP) was multiplied by the ratio of the observed precipitation ($P_{\mathrm{CRU\_XXc}}$) from the Climate Research Unit Time Series (CRU TS) 2.1dataset [48] and the one simulated by the AOGCM ($P_{\mathrm{AOGCM\_XXc}}$), as in Ines & Hansen [49] and Malhi *et al.* [12]:

$$\Delta P'(g,m,i) = \Delta P(g,m,i) \times \frac{P_{\mathrm{CRU\_XXc}}(i, m_{\mathrm{S}}, g_{\mathrm{S}})}{P_{\mathrm{AOGCM\_XXc}}(i, m_{\mathrm{S}}, g_{\mathrm{S}})}. \tag{2.2}$$

In this analysis, the adjustment was performed for each grid box g, month m and AOGCM i, after minimal smoothing in time and space (averaging over the grid box and its immediate neighbourhood: g_{S}, and across three months m_{S}), which significantly limited the number of artefacts caused by division by approximately 0. The remaining few cases of high divergence were capped at 5 and 0.2, based on the analysis of histograms of multiplication factors.

(*c*) *Downscaling of climate-change scenarios*

As a first-order approximation of the potential extent of HTFs in climate regimes defined by 2°C and 4°C of global warming (i.e. initial analysis; before accounting for changes in evapotranspiration), the current forest climatological niche was re-drawn based on high-resolution contemporary climate combined with projected climate-anomaly patterns. The patterns were scaled according to global and land warming in the high-emissions A2 scenario of the Special Report

on Emission Scenarios (SRES) [50]. Whenever possible, the warming data were extracted from the available AOGCM data. Otherwise, they were generated with the above-mentioned simple global thermal model.

Climate patterns, all on the HadCM3 grid, were downscaled with the Worldclim dataset of observed monthly climate [42] on the grid with a high spatial resolution of 2.5′ (approx. 5 km). First, climate patterns representing coastal areas were expanded onto the nearest waters in order to make sure that the change is applied to all coastal areas in the high-resolution dataset. Second, the patterns were re-sampled to higher resolution using the nearest-neighbour method, and smoothed with an average filter. Finally, the resulting coverages with anomalies were added to the Worldclim climatology.

Downscaling is a topic of much debate within the climate modelling community (see [51,52]). The simple approach taken here assumes that the sub-grid patterns and relative magnitudes of rainfall and temperature are preserved under a climate-change pattern. This assumption breaks down if patterns of circulation or moisture transport shift substantially under the climate-change scenario (e.g. the position of orographic or coastal wet spots shifts as wind patterns change). Nevertheless, as a first approximation, such downscaling is useful and of practical importance as it highlights the existence of localized vulnerable or resilient regions in greater detail, something impossible from a low-resolution analysis alone.

(*d*) *Estimating the effect of climate change on ecosystem water use*

The effect of climate change on plant physiology, notably water use, was modelled explicitly using the Integrated Model of Global Effects of Climatic Anomalies (IMOGEN) framework [30,53], which comprises (i) the Met Office Surface Exchange Scheme (MOSES [33]) used in the HadCM3 AOGCM, (ii) the component to emulate the AOGCM simulation's climate pathway (including simple global thermal model), and (iii) the DGVM TRIFFID [33]. The latter component of IMOGEN was switched off; i.e. future changes in the carbon balance of vegetation did not affect the distribution of their functional types. In each run of the framework, the land-surface scheme was forced with atmospheric conditions generated from climate patterns specific to a given AOGCM, which were scaled with the simple climate model according to radiative forcing pathway of the SRES A2 scenario (derived from the Model for the Assessment of Greenhouse-gas Induced Climate Change (MAGICC) model [54,55]) and applied to contemporary climate data CRU TS 2.1. The simple climate model was separately parametrized for each AOGCM, based on the available simulation data; however, the energy balance of the IAP-FGOALS-g1.0 AOGCM could not be reproduced.

The analysis of forest water use focused on 39 grid boxes of the HadCM3 grid that were within the tropics, and were parametrized as having at least 90 per cent cover of broadleaved forest. The combination of climatic drivers and plant physiological responses (the latter through the MOSES land-surface scheme) allowed for the assessment of the importance of each climate variable for evapotranspiration (ET). The results from this assessment were used to adjust the outline of the HTF climatological niche in warmer climate regimes (obtained in the initial assessment) by accounting for the influence of altered evaporative fluxes on plant water stress.

3. Results

(*a*) *Current climatological niche of humid tropical forests*

The analysis of climate-related variables showed that the ones related to ecosystem water stress have the greatest explanatory power for the distribution of HTFs (as inferred from the RMSE), and to some extent, also other vegetation types (as inferred from the deviance). The first five predictors shown in table 1 (see also figure 1) are strongly linked to plant water stress. Annual precipitation, ranked sixth, is the second-best predictor among the Worldclim variables, below dry-season precipitation. Among the temperature-related variables, the strongest predictors were those describing annual-temperature range. However, it should be noted that the relationship between forest cover and low-temperature ranges is probably inverse, with high vegetation cover and transpiration tending to induce low diurnal and annual-temperature range through the surface-energy balance.

The usefulness of climatic variables for this analysis arises not only from their precision in identifying the probability of HTF occurrence in the climate space, as presented above, but also from their ability to distinguish regions of very high and very low probability of the HTF occurrence, which facilitates the creation of a robust map. In terms of such criteria, $MCWD_{100}$, $MCWD_{HTF}$, annual precipitation, PI and dry-season length, are the most robust predictors (see electronic supplementary material), although the last two have considerably lower resolution. Examination of these predictors revealed that the dataset over-predicts some HTF occurrence in high-stress environments, especially in the case of the Americas (probability of HTF occurrence does not reach zero), which is likely to reflect some inaccuracies in the climate and/or land-cover data.

Overall, these results suggest that the spatial distribution of HTFs is best described by their affinity towards high-precipitation regimes with rainfall evenly distributed throughout the year (i.e. low water stress), and they confirm the validity of the principal axes suggested by Malhi *et al.* [12].

Hence, in this study, the HTF niche is also defined through $MCWD_{100}$ (preferred over the similarly robust $MCWD_{HTF}$ that is much more difficult to derive, and PI, which has a lower resolution) and annual precipitation. In addition, mean temperature of the coldest month and mean annual temperature were used to outline the boundary between lowland and montane forests and cool subtropical forests. We assume that change in the temperature range over the twenty-first century will not negatively affect the extent of HTFs, i.e. there is no significant temperature-induced tropical forest 'die-back', and that new areas may enter HTFs conditions as temperatures rise over the low-temperature threshold for HTFs.

Figure 2*a* plots biome dominance in the climatological space defined by $MCWD_{100}$ and annual precipitation. HTFs quantitatively dominate other vegetation types at $MCWD_{100}$ values between −450 and −350 mm. There are some cases where HTFs occupy areas with more negative $MCWD_{100}$ values, but in most cases not as a dominant vegetation type. Along the annual precipitation axis, the vast majority of HTFs dominate at precipitation values above 1500 mm (as indicated by the density contours). In the Americas, there is some dominance of HTF at values below 1500 mm, but this is much less apparent in Africa or Asia.

Table 1. Explanatory power of climate-related variables in terms of the distribution of four major vegetation types across the tropics: HTFs, other forests, dense shrubs and herbs and sparse shrubs and herbs. For each region, the first value is the RMSE of the actual versus predicted probability of HTFs across the variable gradient. The second value (s.d.) is deviance, and it concerns all four vegetation types (low value for dry-season length is because of its very low resolution). The presented ranking was done through averaging of regional RMSE-based ranks. See the electronic supplementary material for the actual and modelled probabilities of vegetation-type occurrence.

		performance as a driver for biome distribution					
		Americas		Africa		Asia	
no.	climate-related variable	RMSE	s.d.	RMSE	s.d.	RMSE	s.d.
1	$MCWD_{HTF}$	0.0769	2.73	0.0304	3.93	0.0448	7.38
2	perhumidity index	0.0784	4.47	0.0312	3.65	0.0433	8.07
3	$MCWD_{100}$	0.0763	5.09	0.0320	2.97	0.0495	7.98
4	precipitation of driest month	0.0533	1.70	0.0253	0.48	0.0886	3.30
5	dry-season length	0.0515	2.14	0.0391	2.74	0.0813	2.49
6	annual precipitation	0.0602	4.24	0.0562	3.72	0.0611	6.92
7	precipitation seasonality[a]	0.0474	2.12	0.0327	5.06	0.1047	7.44
8	annual-temperature range[b]	0.0851	4.51	0.0379	2.90	0.0459	5.38
9	precipitation of driest quarter	0.0590	1.91	0.0214	0.73	0.1060	3.19
10	annual monthly temperature range	0.0987	3.45	0.0566	7.24	0.0520	6.22
11	precipitation of wettest month	0.0485	4.45	0.0770	6.44	0.1350	7.39
12	isothermality[c]	0.0633	3.09	0.0394	8.30	0.1128	17.71
13	precipitation of wettest quarter	0.0503	4.54	0.0840	7.44	0.1556	8.81
14	maximum temperature of warmest month	0.0845	2.66	0.1003	8.81	0.0820	7.43
15	$MCWD_{ET}$	0.0572	3.83	0.0848	10.56	0.1665	9.52
16	mean diurnal temperature range[d]	0.0825	5.45	0.1198	5.30	0.0644	4.78
17	temperature seasonality[e]	0.1266	5.01	0.0578	5.45	0.0652	6.97
18	mean temperature of wettest quarter	0.0931	3.13	0.1039	11.58	0.0782	5.79
19	precipitation of warmest quarter	0.0648	3.16	0.1535	12.80	0.0856	4.31
20	mean temperature of warmest quarter	0.0870	2.88	0.1150	11.35	0.0930	4.20
21	minimum temperature of coldest month	0.0895	4.69	0.1020	6.40	0.1336	11.01
22	annual mean temperature	0.1171	4.94	0.1526	12.82	0.0643	4.67
23	maximum mean temperature of warmest month	0.1334	5.74	0.1082	10.88	0.0902	7.13
24	minimum mean temperature of coldest month	0.1024	4.45	0.1093	13.31	0.2311	17.55
25	annual evapotranspiration (as in $MCWD_{HTF}$)	0.1672	7.47	0.1196	12.47	0.0971	4.94
26	mean temperature of coldest quarter	0.1040	4.34	0.1149	12.20	0.2414	17.86
27	precipitation of coldest quarter	0.1354	5.45	0.2343	11.98	0.0937	3.92
28	mean temperature of driest quarter	0.1120	4.51	0.1230	8.55	0.1907	11.36
29	annual evapotranspiration (as in $MCWD_{ET}$)	0.1125	7.39	0.1513	20.05	0.2440	22.50

[a]Coefficient of variation.
[b]Maximum temperature of warmest month − minimum temperature of coldest month.
[c](Mean diurnal range/annual-temperature range) × 100.
[d]Mean of monthly (maximum mean temperature of warmest month − minimum mean temperature of coldest month).
[e]Standard deviation of monthly temperature series × 100.

The simple outline of the HTF niche (figure 2*b*), defined by one threshold of $MCWD_{100}$ (−350 mm; about 50 mm lower than in Malhi *et al.* [12]) and one of annual precipitation (1500 mm), was found to be a good predictor for the majority of current HTFs distribution. It is apparent that both the $MCWD_{100}$ and precipitation thresholds are useful (i.e. a logical AND combination of both thresholds). Consideration of the $MCWD_{100}$ threshold alone would cause over-prediction of HTF extent in southern Brazil and West and Central Africa (regions with sufficiently weak dry seasons but insufficient recharge in the weak wet season: red zones in figure 2*b*), and consideration of the precipitation threshold alone would cause over-prediction in southeastern Amazonia and peninsular southeast Asia (regions with annual precipitation but very strong dry seasons: light blue zones in figure 2*b*). Therefore, the use of the overlap of the two index-based domains limits their individual shortfalls and makes the potential HTF niche more conservative. This contrasts with the analysis of Malhi *et al.* [12] for Amazonia, which used a logical OR combination of both the thresholds, with either threshold being sufficient for HTFs.

Nevertheless, there were a few regions where HTF extent is over-predicted (purple zones in figure 2*b*), in particular, northwest Amazonia (Colombia and Venezuela) with parts of southern Brazil, and the southwest Congo Basin. The South American mismatch zones partially correspond to seasonal wetlands (the Llanos) where poor surface drainage may prevent HTFs occurrence. The under-prediction in the southwest Congo Basin may be accounted for by radiation: this region has a very cloudy dry season, and hence water demand may be lower than our global analysis indicates—the cloud cover may allow HTFs to persist in drier rainfall regimes than otherwise possible. Deforestation may also be a factor in explaining discrepancies between predicted and observed extent, something very apparent in insular southeast Asia.

Overall, the $MCWD_{100}$- and annual precipitation-based definition appears to be an adequate descriptor of the current spatial extent of HTFs, and was used as a basis for the assessment of the future extent at global warming of 2°C and 4°C.

(*b*) *Changes in the climatological niche at global warming of 2°C and 4°C*

Global warming is expected to alter both the rainfall and temperature regimes, but prognoses for variables that appeared here as important are not equally robust. The predicted changes in precipitation vary between AOGCMs more than the changes in temperature, both in terms of the magnitude and direction of change (table 2), but also the spatial and seasonal distribution, which is of relevance to both annual precipitation and water stress.

Future decreases in precipitation over HTFs of tropical Americas are predicted by seven of the analysed models (approx. 41%), including the well-known extreme scenario from the HadCM3 model. In contrast, precipitation in the other two regions is consistently predicted to increase. The mean rainfall change for each contemporary HTF region at +2°C of global warming is −4, +42 and $+73\,mm\,yr^{-1}$ for South America, Africa and Asia, respectively, and more than twice these amounts at +4°C (table 2). However, the mean change in water stress is greater in tropical Asia than in Africa, owing to differences in the spatial and seasonal distribution of rainfall change predicted by different AOGCMs.

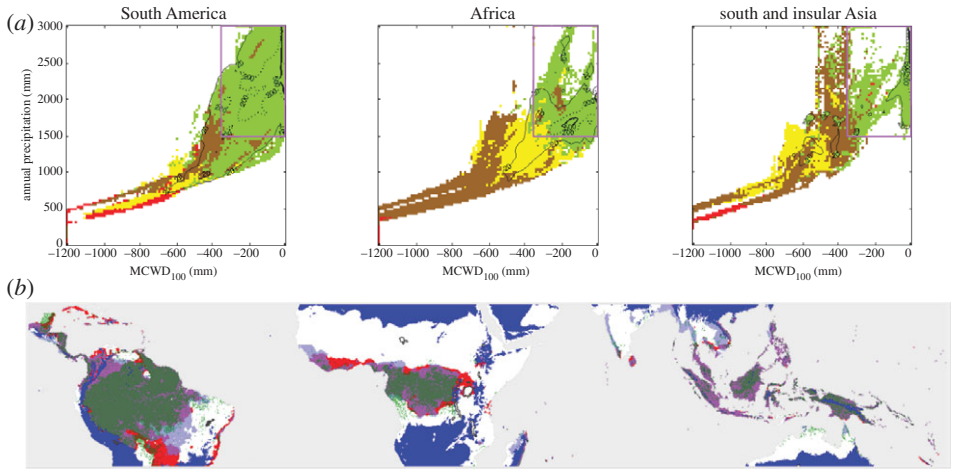

Figure 2. (*a*) Dominance of major tropical vegetation types in a two-dimensional space defined by $MCWD_{100}$ and annual precipitation. Only the cases represented by more than 10 pixels (250 km^2) are plotted. Frequency of HTF pixels is marked with isoclines. The thresholds defining our simple HTF niche (annual precipitation greater than 1500 mm, and $MCWD_{100}$ greater than −350 mm) are delineated by the purple square (green-shaded regions, HTFs; yellow-shaded regions, other forests; brown-shaded regions, dense shrubs and herbaceous; red-shaded regions, sparse shrubs and herbaceous). (*b*) Spatial extent of such HTF niches (in purple), and areas of annual precipitation (light blue) and $MCWD_{100}$ (red) that fall above the proposed thresholds. The current HTF extent is marked in green. Areas too cold for HTFs are marked in dark blue. In mountainous areas adjacent to HTFs they define the boundary between lowland and montane HTFs (green-shaded regions, HTF; light blue-shaded regions, precipitation greater than 1500 mm; red-shaded regions, $MCWD_{ET=100}$ greater than −350 mm; purple-shaded regions, assumed HTF niche; dark blue-shaded regions, low-temperature boundary).

The patterns of future temperature change are much more consistent across AOGCMs than for precipitation, with the largest and smallest increases projected across tropical Americas and Asia, respectively (table 2).

These climate-change patterns imply changes in the extent of the HTF niche, which was re-drawn for each model, first with the assumption that the HTF water demand is not affected by climate change (figure 3). The presented frequencies of particular predictions reflect fractions of AOGCM output which predict that outcome; we do not translate this into a probability of that outcome occurring, as the AOGCM outputs are very unlikely to be distributed evenly across the uncertainty space. With this approach, insular Asia has the smallest risk of retreat of the HTF biome. In the +2°C scenario, the most threatened part of this region is the Indochinese peninsula; in the +4°C scenario, the risk concerning that region increases, and additionally expands to central Sumatra, Sulawesi, India and Philippines, with a maximum of approximately 30 per cent of total niche affected.

The risk for HTF retreat is much more substantial in the case of the tropical Americas, especially in southeastern Amazonia, and around the 'Santarem corridor' of eastern Amazonia. In fact, South America is the only region where models suggest more HTF niche contraction than expansion (see insets in figure 3). In the scenario of +4°C global warming, patterns from the HadCM3 and

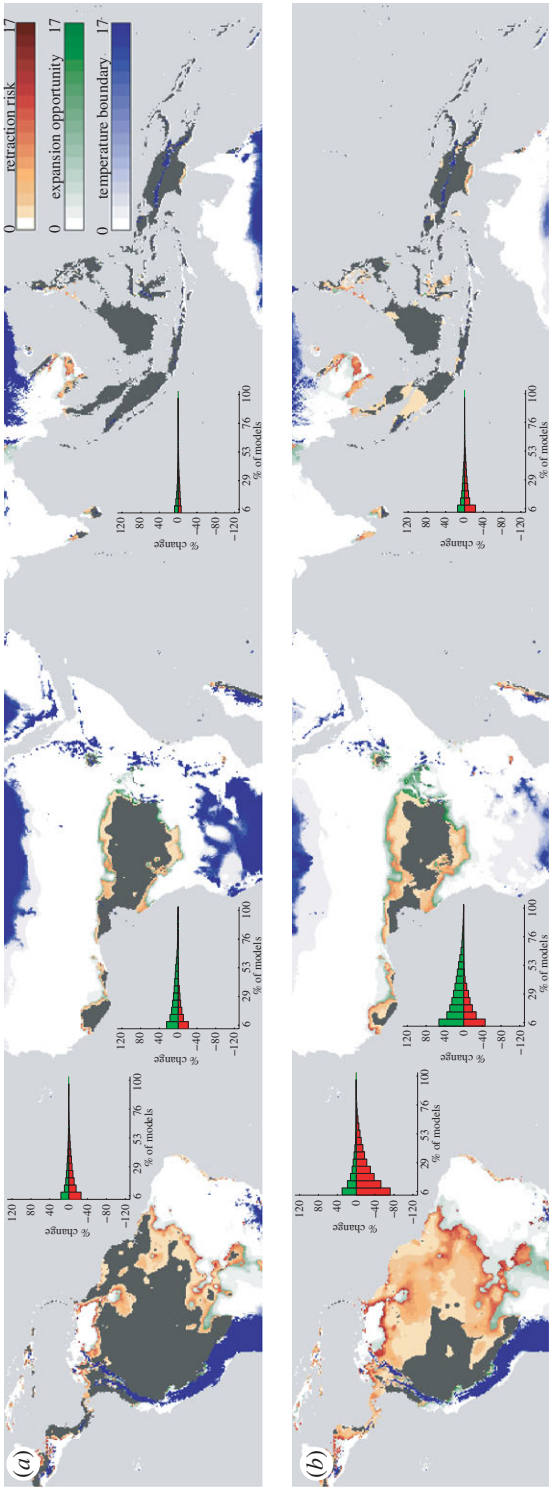

Figure 3. Change in the potential climatological niche of HTFs, as inferred from AOGCM data, assuming no change in ecosystem water demand. (*a*) HTF niche at 2°C and (*b*) 4°C global warming. Dark grey areas mark the niche derived from the current climatological conditions, and are predicted to remain by all AOGCMs. Shades of red and green mark the potential HTF niche contraction and expansion, respectively. Areas too cold for HTFs are marked in blue. In mountainous areas adjacent to HTFs, they define the boundary between lowland and montane tropical forests. Inset bar plots show the percentage of models that agree on a change up to the plotted level.

Table 2. Annual mean temperature, annual precipitation and maximum climatological water stress ($MCWD_{100}$; with and without accounting for climate-change-induced changes in evapotranspiration, ET) in tropical regions inhabited by HTFs, and mean change in these variables at 2°C/4°C of global warming, as derived from AOGCM data. Values are given for regions spatially equivalent to HadCM3 grid boxes that currently support HTFs.

			temperature (2°C/4°C)			annual precipitation (2°C/4°C)			$MCWD_{100}$ (2°C/4°C)			$MCWD_{100}$ + ET change (2°C/4°C)		
no.	GCM	made in	Americas	Africa	Asia	Americas	Africa	Asia	Americas	Africa	Asia	Americas	Africa	Asia
	CRU (contemporary climate)[a]	UK	24.6	24.0	25.2	1952	1585	2021	−287	−322	−353	−287	−322	−353
	WorldClim (contemporary climate)	USA	24.8	24.0	24.8	1983	1553	1990	−208	−270	−283	−208	−270	−283
1	BCCR-BCM2.0[a]	Norway	1.6/3.3	1.6/3.3	1.5/3.2	78/163	71/150	60/127	−3/−24	21/34	7/8	77/102	100/150	86/131
2	CCCMA-CGCM3.1.T47	Canada	1.8/4.3	1.6/3.9	1.5/3.6	−42/−101	31/76	78/189	−23/−73	27/49	13/28	67/69	107/155	91/140
3	CSIRO-MK3.0[a]	Australia	1.9/5.4	1.7/4.6	1.6/4.6	−75/−208	103/287	155/434	−78/−290	2/-39	−26/−134	9/−143	88/89	56/−12
4	CSIRO-MK3.5[a]	Australia	1.9/4.7	1.7/4.2	1.4/3.4	−143/−347	36/88	96/232	−41/−176	−8/−50	−19/−87	49/−48	81/93	63/51
5	GFDL-CM2.0	USA	1.8/4.5	1.6/4.0	1.5/3.8	−50/−124	5/12	33/82	−24/−92	19/37	−1/−14	62/62	104/161	79/105
6	GFDL-CM2.1	USA	1.9/4.5	1.9/4.5	1.6/3.9	23/54	16/38	9/21	−23/−64	9/10	−16/−44	61/69	92/137	65/88
7	GISS-EH	USA	1.7/4.2	1.8/4.5	1.6/3.8	112/274	58/141	38/94	11/15	14/27	−12/−20	87/126	100/152	68/93
8	IAP-FGOALS-g1.0	China	1.9/4.5	2.0/4.8	1.7/4.1	10/24	24/58	82/202	−10/−37	24/42	−24/−89	73/82	108/141	57/30
9	INM-CM3.0[a]	Russia	1.5/3.6	1.6/3.9	1.5/3.5	165/401	37/91	34/82	−12/−64	34/36	−11/−66	71/68	115/153	67/68
10	IPSL-CM4	France	1.7/4.1	1.6/4.0	1.6/3.9	66/162	1/1	66/161	−3/−37	17/25	−5/−17	76/92	105/157	73/109
11	MIROC3.2 (hires)[a]	Japan	1.7/4.2	1.5/3.8	1.5/3.6	19/45	16/39	50/123	2/−20	18/33	10/12	81/105	103/153	88/129
12	MIROC3.2 (medres)[a]	Japan	1.9/4.5	1.5/3.5	1.4/3.3	28/69	85/206	71/172	−6/−30	54/92	8/15	75/100	131/184	86/131
13	MPI-ECHAM5	Germany	1.9/4.6	1.7/4.2	1.6/3.9	−16/−39	78/187	124/297	−23/−73	7/11	1/−1	62/72	95/142	81/120
14	NCAR-CCSM3.0	USA	1.5/3.6	1.2/2.9	1.3/3.2	69/169	78/189	84/203	−15/−50	46/93	13/29	69/88	123/194	90/141
15	NCAR-PCM1	USA	1.4/3.5	1.3/3.4	1.5/3.8	45/114	2/4	75/192	1/−20	7/−1	8/3	79/99	98/136	87/133
16	UKMO-HadCM3	UK	2.3/5.7	1.7/4.2	1.7/4.1	−234/−582	35/86	94/234	−86/−317	23/38	−18/−69	13/−133	106/149	64/73
17	UKMO-HadGEM1	UK	1.8/4.3	1.7/4.2	1.5/3.7	−125/−305	41/99	89/218	−33/−143	0/−8	5/6	57/10	89/134	84/132
	mean		1.8/4.3	1.6/4.0	1.5/3.7	−4/−14	42/103	73/180	−21/−88	19/25	−4/−26	63/48	103/146	76/98

[a]Data on minimum and maximum monthly temperature is available.

CSIRO Mk 3.0 models imply a retreat of the majority of Amazonian HTFs (up to 80% of current HTF extent in the tropical American region), and patterns from seven models (41% of the dataset) predict at least a 10 per cent contraction of HTF extent. The northeastern coast of Amazonia is partly buffered from this risk because of the locally high rainfall at the oceanic boundary (at least at +2°C), a feature that is not apparent in lower resolution climate-model output. The forest zone of Central America and the Caribbean region (Yucatan, Guatemala, Honduras, Cuba) also shows high probability of forest retreat. The severity of the predicted HTF niche contraction, especially in the case of South America, depends on the adjustment procedure, which calibrates precipitation patterns according to each AOGCM's skill to reproduce the contemporary precipitation regime. Figures S2 and S3 in the electronic supplementary material present scenarios generated with precipitation patterns without adjustment, which lead to a somewhat smaller HTF niche contraction.

The scenario of forest expansion in some parts of Africa is the most robust among all regional projections (>80% of models predict some expansion). In the +2°C scenario, the HTF niche in the Congo Basin shows relatively little movement, with equally likely changes in both directions predicted mainly at the fringes. Data from one model predicts the possibility of substantial retreat of Congo Basin HTFs (up to approx. 20% of total area), but there also appears to be potential for eastward expansion of the humid forest niche north of Lake Victoria. The expansion scenario becomes very widespread in the +4°C scenario (up to approx. 50% of the current HTF area), whereas at the same time in the Congo Basin, the risk of forest retreat becomes substantial, with three models (approx. 18%) agreeing on up to 15 per cent contraction, almost leading to the split of the continuous block of forest cover into separate eastern and western parts. Three models suggest substantial contraction of west African HTF extent, leading to possible fragmentation of the upper Guinean forest zone.

Analysis of the temperature-related boundary of lowland HTFs shows that areas currently too cold to sustain HTFs in Africa and Asia may contract substantially, even in the +2°C scenario. In many cases, the current temperature boundary delineates the transition between the lowland and montane HTFs. Although the actual position of this boundary is very sensitive to downscaling of climate patterns, in some cases, the potential of lowland forests to encroach onto montane forests is manifested as large mountainous areas become warmer, for example in some parts of the eastern Andes.

(*c*) *The effect of decreased ecosystem water use*

The climate-induced change in ET, modelled with the land-surface scheme of the HadCM3 AOGCM, was approximated through the change in atmospheric CO_2, which was relatively well correlated with AET anomalies ($R^2 = 0.25$) of the pooled emulated 'SRES A2' AOGCM climate pathways. Across the simulations, the ET decreased steadily over time, reaching about 25 mm month^{-1} total decrease near year 2100 (figure 4*b*,*c*). On the other hand, the net primary production (NPP; figure 4*a*), reflecting the overall HTF functioning, was much more variable throughout the runs, and in general it first increased, and then started to decline at various points in time and with varying speed. The lowest NPP occurred at the highest temperatures, although the NPP drop below the

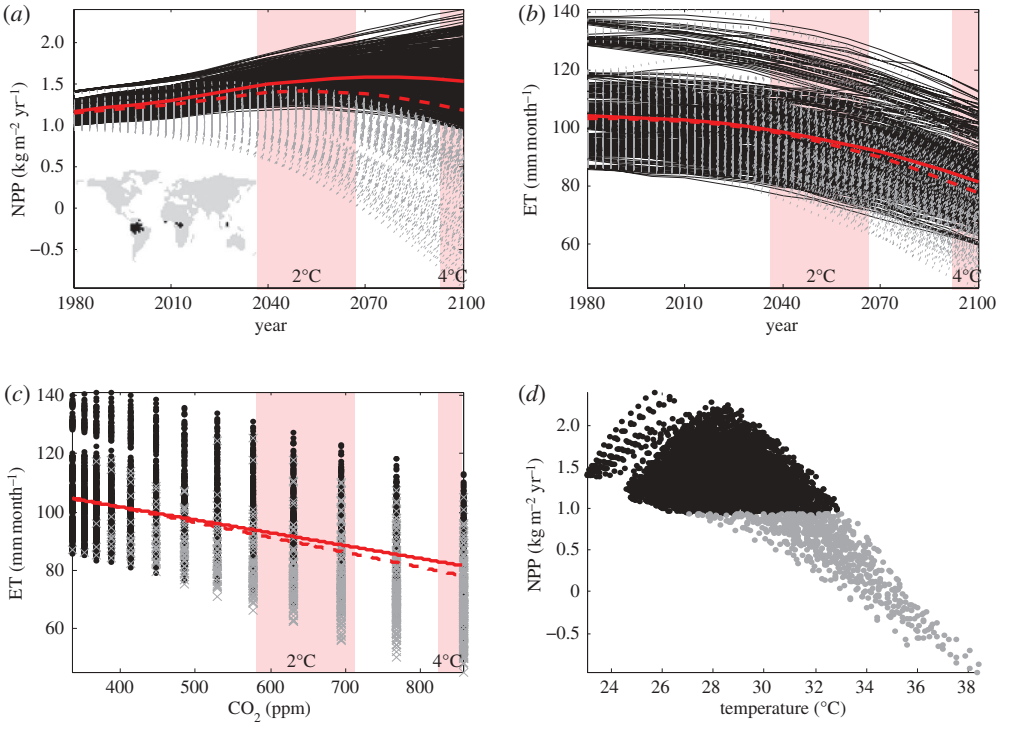

Figure 4. (*a*) Changes in the NPP of HTFs across SRES A2 scenario simulated with land-surface scheme and climate-change patterns from 16 AOGCM runs. The 39 considered grid boxes are situated within tropics (see inset map) and are covered by broadleaved forests in at least 90%. Red solid curve marks an average of pathways in which NPP does not drop below minimum contemporary levels (marked in solid black). The dashed red curve is an average of all cases (including the pathways reaching low NPP values, which are marked in grey). (*b*) Corresponding changes in evapotranspiration; red curves have the same role as in (*a*). (*c*) Relationship between the atmospheric CO_2 concentration and evapotranspiration, with regression lines marked in red. (*d*) NPP plotted against monthly mean temperature.

minimum contemporary levels occurred at varying temperatures, so any specific temperature threshold for HTF functioning could not be established (figure 4*c*). These results are generally consistent with the simple approach to delineate the HTF niche, and the appearance of some risk of die-back at the +2°C scenario, which in some areas becomes substantial at the +4°C scenario. In order to avoid confusing the ET decrease that reflects better plant water efficiency in the CO_2-enriched atmosphere, with the ET decrease induced by the declining NPP, all pathways with NPP that fell below the minimum contemporary levels were excluded from the analysis.

Taking into account the possible decrease in ecosystem water demand drastically changed the estimates of the HTF potential niche in the future (figure 5), overall shifting the scenarios towards potential forest expansion. At +2°C, the scenario of severe niche contraction in South America is offset by the potential niche expansion southeastwards. In Africa, the potential for expansion markedly prevails over the contraction. Finally, there is a small potential for niche expansion in continental south Asia (i.e. expansion of humid forest into monsoonal

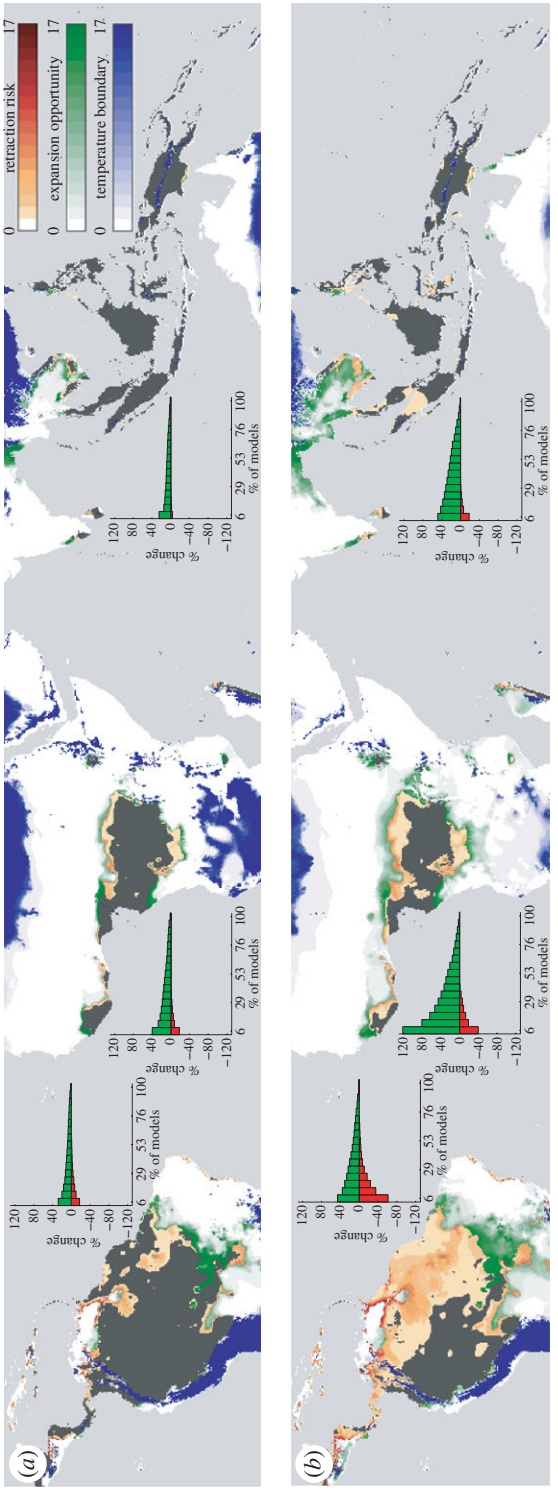

Figure 5. Change in the potential climatological niche of HTFs, as inferred from AOGCM data. (*a*) HTF niche at 2°C and (*b*) 4°C global warming. This scenario accounts for the decrease in ecosystem water demand in new climate regimes, modelled in the land-surface scheme (see also figure 4). Dark grey areas mark the niche derived from the current climatological conditions, and are predicted to remain by all AOGCMs. Shades of red and green mark the potential HTF niche contraction and expansion, respectively. Areas too cold for HTFs are marked in blue. In mountainous areas adjacent to HTFs, they define the boundary between lowland and montane tropical forests. Inset bar plots show the percentage of models that agree on a change up to the plotted level.

forest zone). At +4°C, the risk of climate-induced deforestation in Amazonia is still apparent (four models, or 24% of the dataset), and in the most pessimistic scenario (HadCM3), it surpasses the potential for expansion. In addition, parts of Central America and the Caribbean still show a substantial risk of forest retreat. In Africa, the potential expansion of forest area around the Congo Basin increases, although the risk of niche contraction remains, mainly at the north and south. Moreover, large new areas in west Africa and Madagascar appear as potentially suitable for expansion. In Asia, the risk of forest die-back in the Philippines is reduced, but remains in central Sumatra (one model) and Sulawesi (two models). Moreover, there is an increased potential for expansion of the HTF niche into the seasonal (monsoonal) forest area of mainland southeast Asia and eastern India.

4. Discussion

The presented results show that the distribution of HTFs can be fairly well characterized by the rainfall regime, in particular the plant water deficit. This was reflected by the relative explanatory strength of tested climate-related variables. The findings were generally consistent across the three tropical regions; however, on average, the predictors of vegetation classes performed best across the African region, where all major vegetation classes are well represented and relatively well preserved, and strong wet–dry gradients lead to delineation of sharper boundaries of the HTFs biome. Confusion in classification of remotely sensed data, inaccuracies in interpolated climate data, and bias owing to pixel aggregation can also be expected to play a role. In fact, some of the findings seem to confirm the presence of some flaws in the dataset used; for example, the apparent presence of some HTFs in high water-stress environments.

Precipitation change is among the aspects of climate change that are the most difficult to predict [56]. This problem is reflected by large differences in the derived precipitation-change patterns, and by the varying skill of AOGCMs to reproduce contemporary precipitation regime, which in turn also has an impact on the magnitude of the predicted patterns of change. The latter is well exemplified by the discrepancy between the HTF extent estimated with precipitation patterns adjusted for the AOGCM bias (main results) and not adjusted (electronic supplementary material). Our analysis demonstrates the likely spatially complex pattern of the HTF response to climate change, which is not captured by low-resolution modelling frameworks, though the pattern's exact form is highly dependent on the quality of current climatological data, and on the downscaling method. At fine spatial scales, there is often greater potential for the persistence of HTFs in part of the landscape or region. The fine scale also enables better representation of spatially variable vulnerability to drought. In contrast, some aspects of the HTFs response to climate change are much more spatially uniform, such as the considered increase in water-use efficiency in the atmosphere richer in CO_2. Such factors make the pattern of the future HTFs occurrence more spatially consistent.

The climatological niche presented in this study is a simple, but scalable, model of the environmental space inhabited by HTFs. This model does not include non-climatic factors like soil fertility, soil hydrology and relief, which can play a role in both the contemporary and future distribution of HTFs. Moreover, the model is

based on climatic means, which do not fully capture the frequency of occasional dry periods that have a strong effect on biome boundaries. Hence, the presented spatial patterns in the HTF niche extent should be interpreted as a visualization of basic mechanisms governing the change, rather than exact predictions of the actual forest cover. The results could also be interpreted in the context of the changing fire risk, as well as the uncertain plant physiological response to higher temperatures. These two aspects of future HTF distribution are discussed below, as they were not included in the construction of the presented maps.

The expansion of the potential HTF niche requires cautious interpretation. First, actual migration and colonization of non-HTF regions may well lag behind expansion of the potential niche, as processes of dispersion and competition play out. Second, in practice, the expansion often means migration of forest into areas already heavily deforested and cultivated, where heavy anthropogenic pressure will preclude it. Third, expansion of HTFs into dry forest, savanna or grassland is not without consequences for the retreating dry ecosystem, which can host high and unique biodiversity, and may be more threatened by anthropogenic pressures than the HTF biome (for example, the high biodiversity and highly threatened cerrado biome of Brazil or the savannas of east Africa). This study highlights regions where the interactions of climate change with land-use change may be strong (especially, east Amazonia and west Africa), and the nature of these interactions needs to be explored in greater detail for each sensitive region (e.g. [12]).

The simulations performed with the land-surface scheme have shown that high CO_2 may cause an increase in ecosystem water-use efficiency, and greater HTF resilience in drier rainfall regimes, which in turn decreases the risk of the potential niche contraction, and in some regions, translates to its significant expansion. It seems likely that if this analysis had also incorporated impacts on altered photosynthesis and respiration on plant competition, the CO_2-enriched environment would favour further forest expansion into C4 grasslands. On the other hand, increased temperatures could potentially favour retreat of HTF extent at the expense of grasslands, but this depends critically on how close tropical forests are to a high-temperature threshold. South American HTFs have the greatest risk of facing dangerous temperatures, as the rates of warming over this region are predicted to be the highest of any tropical region.

The vulnerability of tropical trees to future warming is uncertain and controversial [21,57]. The maximal temperatures may be important for the forest survival if they approach levels at which enzymes responsible for photosynthesis are denatured (around 45°C; [18,58]). Lloyd & Farquhar [21] argue that tropical forests will not exceed their optimal temperature ranges, whereas Clark *et al.* [57] suggest reduced photosynthesis or increased plant respiration in response to short-term warming. The temperature sensitivities of both photosynthesis and respiration can change, and there are ecophysiological arguments that plants can acclimate to a warming of a few degrees [59,60]. However, there are very few empirical data on the degree to which tropical trees respond and are able to acclimate to increased temperatures and drought [61–63]. Several contemporary dynamic vegetation models may be overly sensitive to temperature and not allowing for acclimation effects [31]. Other components of the ecosystem, however, such as insect pollinators, may be more vulnerable to a small warming (e.g. [64]), with knock-on effects for forest-plant communities.

Moreover, warming increases the risk of fire [12,27]. In a complementary study, Le Page *et al.* [65] project the potential area under threat from future biomass burning. Whereas the physiological effects lead to reduced plant water use, through reductions in plant transpiration, fire danger is linked to dead fuel moisture and thus evaporation. Therefore, although plant physiology acts to mitigate the effects of warming on the potential forest extent, these forests may be more susceptible to future forest fire. If the effects of temperature on fire risk and photosynthesis were included in the presented analysis, it could be expected that the distribution of HTFs may be more constrained than that presented here, especially in areas exposed to anthropogenic fire ignition (South America, insular Asia).

Precipitation and temperature patterns appear as crucial factors determining plant functioning and the type of vegetation cover, as they are directly linked to the availability of (soil) water and (thermal) energy that influence photosynthesis and respiration. However, there may be other aspects of water and energy availability that are also relevant. In practice, these are often more complex and more difficult to map. For example, atmospheric humidity is an important ecological factor in tropical forest areas because of its effect on evapotranspiration, and hence photosynthetic rates of plants. The saturation deficit pattern of HTF areas contrasts with those of both seasonal and montane forest areas in the tropics [16]. Another potentially critical variable, net radiation, is the strongest predictor of the spatial pattern of evapotranspiration over the humid tropics [15,66], and is linked with the intensity of photosynthesis both directly (via photosynthetically active radiation; PAR) and indirectly (via thermal radiation). Changes in the ratio between diffuse and direct radiation, perhaps because of biomass burning haze, can alter canopy light penetration and overall canopy photosynthesis [21,67]. These, and other, variables may covary with precipitation and temperature, and their importance could become apparent in new climate regimes. The definition of the future climatological niche of the HTFs could be extended by incorporating some of the above factors, but such an extension is beyond the scope of this study.

Climate-change-driven shifts in the extent of tropical forests represent a risk for policies concerned with biodiversity loss and climate change, including the reduced emissions from deforestation and forest degradation (REDD [68]) discussed under the United Nations framework convention for climate change. The scheme is meant to exploit the potential to mitigate climate change through the protection of forests' carbon pool (and biodiversity—as a co-benefit [69]), but its success will depend on the long-term forest resilience. Direct deforestation and uncontrolled fire already undermine forest permanence [70]. In comparison, the risk of climate-induced die-back seems only hypothetical. However, this risk is potentially a critical one because its cause, once present, cannot be addressed on short time scales owing to the climate system's inertia.

In conclusion, water availability is the best determinant of the current distribution of HTFs, which can dominate over other vegetation types only in high-precipitation, low water-stress environments. Because climate models differ in their predictions of future precipitation regime, change in the extent of the HTF niche is uncertain. However, the risks and opportunities are not evenly distributed and some patterns emerge from the ensemble of models used. For example, Amazonian forests seem relatively more likely to experience some decrease in precipitation, and a few models suggest extensive possibility of retreat of the

HTF niche, or 'die-back'. In contrast, the majority of HTFs in South and Insular Asia are not predicted to face climate-driven die-back. In Africa, there is potential for both HTF contraction and expansion. In all regions, the potential to expand is due to both the more favourable precipitation regime, and the retreat of the low-temperature threshold. If CO_2 has an effect on water balance as predicted, then the expansion of the HTF niche is more likely than the contraction. In practice, in many places with high agricultural pressure, it is more plausible for HTFs to be locally destroyed than naturally colonize new areas, although apparent forest expansion and woody encroachment has been reported in many areas of Africa. Future extent of HTFs may also be controlled by other factors, for example, critically high temperatures, which are not yet fully understood.

While this study has its limitations by not incorporating fully the (poorly understood) physiological responses to temperature (although some temperature effect is implicit in the CO_2 effect on water-use efficiency), it makes an important contribution in highlighting areas of potential risk and resilience to climate change, and incorporating multiple climate models and high-resolution climatology. The presented approach is a step towards a more biodiversity- and conservation-relevant interpretation of the climate modelling results. Future improvements to the approach could include higher resolution climate patterns, more complex HTF niches, more sophisticated downscaling, and sensitivity analysis to the critical temperatures and acclimation rates.

The authors thank David Galbraith, Toby Marthews and Marta Szulkin for comments, Dan Bebber for advice on statistical analysis, and Gil Lizcano for technical support. Comments from two anonymous reviewers and the editor greatly improved the manuscript. We acknowledge the modelling groups, the Program for Climate Model Diagnosis and Intercomparison, and the World Climate Research Programme (WCRP) Working Group on Coupled Modelling for their roles in making available the WCRP Coupled Model Intercomparison Project 3 multi-model dataset.

References

1 Mayaux, P., Holmgren, P., Achard, F., Eva, H., Stibig, H. & Branthomme, A. 2005 Tropical forest cover change in the 1990s and options for future monitoring. *Phil. Trans. R. Soc. B* **360**, 373–384. (doi:10.1098/rstb.2004.1590)

2 Dirzo, R. & Raven, P. H. 2003 Global state of biodiversity and loss. *Annu. Rev. Environ. Resour.* **28**, 137–167. (doi:10.1146/annurev.energy.28.050302.105532)

3 van der Werf, G. R., Morton, D. C., DeFries, R. S., Olivier, J. G. J., Kasibhatla, P. S., Jackson, R. B., Collatz, G. J. & Randerson, J. T. 2009 CO_2 emissions from forest loss. *Nat. Geosci.* **2**, 737–738. (doi:10.1038/ngeo671)

4 Lewis, S. L., Lloyd, J., Sitch, S., Mitchard, E. T. A. & Laurance, W. F. 2009 Changing ecology of tropical forests: evidence and drivers. *Annu. Rev. Ecol. Evol. Syst.* **40**, 529–549. (doi:10.1146/annurev.ecolsys.39.110707.173345)

5 ter Steege, H. *et al* 2003 A spatial model of tree alpha-diversity and tree density for the Amazon. *Biodivers. Conserv.* **12**, 2255–2277. (doi:10.1023/A:1024593414624)

6 Saatchi, S. S., Houghton, R. A., Alvala, R., Soares, J. V. & Yu, Y. 2007 Distribution of aboveground live biomass in the Amazon basin. *Glob. Change Biol.* **13**, 816–837. (doi:10.1111/j.1365-2486.2007.01323.x)

7 Baccini, A., Laporte, N., Goetz, S. J., Sun, M. &Dong, H. 2008 A first map of tropical Africa's above-ground biomass derived from satellite imagery. *Environ. Res. Lett.* **3**, 045011. (doi:10.1088/1748-9326/3/4/045011)

8 FAO. 2001 Global Forest Resources Assessment 2000. FAO forestry paper 140. Rome, Italy: FAO.

9 FAO. 2006 Global Forest Resources Assessment 2005. FAO forestry paper 147. Rome, Italy: FAO.

10 Prentice, K. C. 1990 Bioclimatic distribution of vegetation for general-circulation model studies. *J. Geophys. Res. Atmos.* **95**, 11 811–11 830. (doi:10.1029/JD095iD08p11811)

11 Lewis, S. L. 2006 Tropical forests and the changing earth system. *Phil. Trans. R. Soc. B* **361**, 195–210. (doi:10.1098/rstb.2005.1711)
12 Malhi, Y., Aragao, L., Galbraith, D., Huntingford, C., Fisher, R., Zelazowski, P., Sitch, S., McSweeney, C. & Meir, P. 2009 Exploring the likelihood and mechanism of a climate-change-induced dieback of the Amazon rainforest. *Proc. Natl Acad. Sci. USA* **106**, 20 610–20 615. (doi:10.1073/pnas.0804619106)
13 Kumagai, T. *et al.* 2005 Annual water balance and seasonality of evapotranspiration in a Bournean tropical rainforest. *Agric. For. Meteorol.* **128**, 81–92. (doi:10.1016/j.agrformet.2004.08.006)
14 Malhi, Y., Pegoraro, E., Nobre, A. D., Pereira, M. G. P., Grace, J., Culf, A. D. & Clement, B. 2002 Energy and water dynamics of a central Amazonian rain forest. *J. Geophys. Res.* **107**, 8061. (doi:10.1029/2001JD000623)
15 Fisher, J. B. *et al.* 2009 The land–atmosphere water flux in the tropics. *Glob. Change Biol.* **15**, 2694–2714. (doi:10.1111/j.1365-2486.2008.01813.x)
16 Richards, P. W., Walsh, R. P. D., Baillie, I. C. & Greig-Smith, P. 1996 *The tropical rain forest.* Cambridge, UK: Cambridge University Press.
17 Walsh, R. P. D. 1992 Representation and classification of tropical climates for ecological purposes using the perhumidity index. *Swansea Geogr.* **24**, 109–129.
18 Betts, R. A., Collins, M., Hemming, D. L., Jones, C. D., Lowe, J. A. & Sanderson, M. G. 2011 When could global warming reach 4°C? *Phil. Trans. R. Soc. A* **369**, 67–84. (doi:10.1098/rsta.2010.0292)
19 Cox, P. M., Betts, R. A., Jones, C. D., Spall, S. A. & Totterdell, I. J. 2000 Acceleration of global warming due to carbon-cycle feedbacks in a coupled climate model. *Nature* **408**, 184–187. (doi:10.1038/35041539)
20 Lewis, S. L., Malhi, Y. & Phillips, O. L. 2004 Fingerprinting the impacts of global change on tropical forests. *Phil. Trans. R. Soc. Lond. B* **359**, 437–462. (doi:10.1098/rstb.2003.1432)
21 Lloyd, J. & Farquhar, G. D. 2008 Effects of rising temperatures and [CO_2] on the physiology of tropical forest trees. *Phil. Trans. R. Soc. B* **363**, 1811–1817. (doi:10.1098/rstb.2007.0032)
22 White, A., Cannell, M. G. R. & Friend, A. D. 1999 Climate change impacts on ecosystems and the terrestrial carbon sink: a new assessment. *Glob. Environ. Change Hum. Policy Dimens.* **9**, S21–S30. (doi:10.1016/S0959-3780(99)00016-3)
23 Betts, R. A., Cox, P. M., Collins, M., Harris, P. P., Huntingford, C. & Jones, C. D. 2004 The role of ecosystem–atmosphere interactions in simulated Amazonian precipitation decrease and forest dieback under global climate warming. *Theor. Appl. Climatol.* **78**, 157–175. (doi:10.1007/s00704-004-0050-y)
24 Cox, P. M., Betts, R. A., Collins, M., Harris, P. P., Huntingford, C. & Jones, C. D. 2004 Amazonian forest dieback under climate-carbon cycle projections for the 21st century. *Theor. Appl. Climatol.* **78**, 137–156. (doi:10.1007/s00704-004-0049-4)
25 Huntingford, C. *et al.* 2008 Towards quantifying uncertainty in predictions of Amazon 'dieback'. *Phil. Trans. R. Soc. B* **363**, 1857–1864. (doi:10.1098/rstb.2007.0028)
26 Lenton, T. M., Held, H., Kriegler, E., Hall, J. W., Lucht, W., Rahmstorf, S. & Schellnhuber, H. J. 2008 Tipping elements in the Earth's climate system. *Proc. Natl Acad. Sci. USA* **105**, 1786–1793. (doi:10.1073/pnas.0705414105)
27 Poulter, B., Aragão, L., Heyder, U., Gumpenberger, M., Heinke, J., Langerwisch, F., Rammig, A., Thonicke, K. & Cramer, W. 2010 Net biome production of the Amazon basin in the 21st Century. *Glob. Change Biol.* **16**, 2062–2075. (doi:10.1111/j.1365-2486.2009.02064.x)
28 Cramer, W. *et al.* 2001 Global response of terrestrial ecosystem structure and function to CO_2 and climate change: results from six dynamic global vegetation models. *Glob. Change Biol.* **7**, 357–373. (doi:10.1046/j.1365-2486.2001.00383.x)
29 Sitch, S. *et al.* 2008 Evaluation of the terrestrial carbon cycle, future plant geography and climate-carbon cycle feedbacks using five Dynamic Global Vegetation Models (DGVMs). *Glob. Change Biol.* **14**, 2015–2039. (doi:10.1111/j.1365-2486.2008.01626.x)
30 Huntingford, C., Harris, P. P., Gedney, N., Cox, P. M., Betts, R. A., Marengo, J. A. & Gash, J. H. C. 2004 Using a GCM analogue model to investigate the potential for Amazonian forest dieback. *Theor. Appl. Climatol.* **78**, 177–185. (doi:10.1007/s00704-004-0051-x)

31 Galbraith, D., Levy, P. E., Sitch, S., Huntingford, C., Cox, P., Williams, M. & Meir, P. 2010 Multiple mechanisms of Amazonian forest biomass losses in three dynamic global vegetation models under climate change. *New Phytol.* **187**, 647–665. (doi:10.1111/j.1469-8137.2010.03350.x)

32 Cox, P. M. 2001 Description of the TRIFFID dynamic global vegetation model. Technical note 24. Bracknell, UK: Hadley Centre, Met office.

33 Cox, P. M., Huntingford, C. & Harding, R. J. 1998 A canopy conductance and photosynthesis model for use in a GCM land surface scheme. *J. Hydrol.* **213**, 79–94. (doi:10.1016/S0022-1694(98)00203-0)

34 Schaphoff, S., Lucht, W., Gerten, D., Sitch, S., Cramer, W. & Prentice, I. C. 2006 Terrestrial biosphere carbon storage under alternative climate projections. *Clim. Change* **74**, 97–122. (doi:10.1007/s10584-005-9002-5)

35 Scholze, M., Knorr, W., Arnell, N. W. & Prentice, I. C. 2006 A climate-change risk analysis for world ecosystems. *Proc. Natl Acad. Sci. USA* **103**, 13 116–13 120. (doi:10.1073/pnas.0601816103)

36 Salazar, L. F., Nobre, C. A. & Oyama, M. D. 2007 Climate change consequences on the biome distribution in tropical South America. *Geophys. Res. Lett.* **34**, L09708. (doi:10.1029/2007GL029695)

37 Lapola, D. M., Oyama, M. D. & Nobre, C. A. 2009 Exploring the range of climate biome projections for tropical South America: the role of CO_2 fertilization and seasonality. *Glob. Biogeochem. Cycles* **23**, GB3003. (doi:10.1029/2008GB003357)

38 Cook, K. H. & Vizy, E. K. 2008 Effects of twenty-first-century climate change on the Amazon rain forest. *J. Clim.* **21**, 542–560. (doi:10.1175/2007JCLI1838.1)

39 Trivedi, M. R., Berry, P. M., Morecroft, M. D. & Dawson, T. P. 2008 Spatial scale affects bioclimate model projections of climate change impacts on mountain plants. *Glob. Change Biol.* **14**, 1089–1103. (doi:10.1111/j.1365-2486.2008.01553.x)

40 Willis, K. J. & Bhagwat, S. A. 2009 Biodiversity and climate change. *Science* **326**, 806–807. (doi:10.1126/science.1178838)

41 Bartholome, E. & Belward, A. S. 2005 GLC2000: a new approach to global land cover mapping from Earth observation data. *Int. J. Remote Sens.* **26**, 1959–1977. (doi:10.1080/01431160412331291297)

42 Hijmans, R. J., Cameron, S. E., Parra, J. L., Jones, P. G. & Jarvis, A. 2005 Very high resolution interpolated climate surfaces for global land areas. *Int. J. Climatol.* **25**, 1965–1978. (doi:10.1002/joc.1276)

43 Fisher, J. B., Tu, K. P. & Baldocchi, D. D. 2008 Global estimates of the land–atmosphere water flux based on monthly AVHRR and ISLSCP-II data, validated at 16 FLUXNET sites. *Remote Sens. Environ.* **112**, 901–919. (doi:10.1016/j.rse.2007.06.025)

44 Mitchell, J. F. B., Johns, T. C., Eagles, M., Ingram, W. J. & Davis, R. A. 1999 Towards the construction of climate change scenarios. *Clim. Change* **41**, 547–581. (doi:10.1023/A:1005466909820)

45 Huntingford, C. & Cox, P. M. 2000 An analogue model to derive additional climate change scenarios from existing GCM simulations. *Clim. Dyn.* **16**, 575–586. (doi:10.1007/s003820000067)

46 Wigley, T. M. L., Raper, S. C. B., Hulme, M. & Smith, S. 2000 The MAGICC/SCENGEN climate scenario generator, version 2.4, technical manual. Climatic Research Unit, University of East Anglia, Norwich, UK.

47 Cabre, M. F., Solman, S. A. & Nuñez, M. N. 2010 Creating regional climate change scenarios over southern South America for the 2020's and 2050's using the pattern scaling technique: validity and limitations. *Clim. Change* **98**, 449–469. (doi:10.1007/s10584-009-9737-5)

48 Mitchell, T. D. & Jones, P. D. 2005 An improved method of constructing a database of monthly climate observations and associated high-resolution grids. *Int. J. Climatol.* **25**, 693–712. (doi:10.1002/joc.1181)

49 Ines, A. V. M. & Hansen, J. W. 2006 Bias correction of daily GCM rainfall for crop simulation studies. *Agric. For. Meteorol.* **138**, 44–53. (doi:10.1016/j.agrformet.2006.03.009)

50 Nakicenovic, N. *et al.* 2000 *IPCC special report on emission scenarios*. Cambridge, UK: Cambridge University Press.

51 Baron, C., Sultan, B., Balme, M., Sarr, B., Traore, S., Lebel, T., Janicot, S. & Dingkuhn, M. 2005 From GCM grid cell to agricultural plot: scale issues affecting modelling of climate impact. *Phil. Trans. R. Soc. B* **360**, 2095–2108. (doi:10.1098/rstb.2005.1741)
52 Fowler, H. J., Blenkinsop, S. & Tebaldi, C. 2007 Linking climate change modelling to impacts studies: recent advances in downscaling techniques for hydrological modelling. *Int. J. Climatol.* **27**, 1547–1578. (doi:10.1002/joc.1556)
53 Huntingford, C. *et al.* 2007 IMOGEN: an intermediate complexity climate model to evaluate terrestrial impacts of a changing climate. *Geosci. Model Dev. Discuss.* **3**, 1161–1184. (doi:10.5194/gmdd-3-1161-2010)
54 Hulme, M., Raper, S. C. B. & Wigley, T. M. L. 1995 An integrated framework to address climate-change (escape) and further developments of the global and regional climate modules (magicc). *Energy Policy* **23**, 347–355. (doi:10.1016/0301-4215(95)90159-5)
55 Meinshausen, M., Raper, S. C. B. & Wigley, T. M. L. 2008 Emulating IPCC AR4 atmosphere–ocean and carbon cycle models for projecting global-mean hemispheric and land/ocean temperature: MAGICC 6.0. *Atmos. Chem. Phys.* **8**, 6153–6272. (doi:10.5194/acpd-8-6153-2008)
56 Schiermeier, Q. 2010 The real holes in climate science. *Nature* **463**, 284–287. (doi:10.1038/463284a)
57 Clark, D. A. 2004 Sources or sinks? The responses of tropical forests to current and future climate and atmospheric composition. *Phil. Trans. R. Soc. Lond. B* **359**, 477–491. (doi:10.1098/rstb.2003.1426)
58 Sung, D.-Y., Kaplan, F., Lee, K.-J. & Guy, C. L. 2003 Acquired tolerance to temperature extremes. *Trends Plant. Sci.* **8**, 179–187. (doi:10.1016/S1360-1385(03)00047-5)
59 Atkin, O. K., Bruhn, D., Hurry, V. M. & Tjoelker, M. G. 2005 The hot and the cold: unravelling the variable response of plant respiration to temperature. *Funct. Plant Biol.* **32**, 87–105. (doi:10.1071/FP03176)
60 Kattge, J. & Knorr, W. 2007 Temperature acclimation in a biochemical model of photosynthesis: a reanalysis of data from 36 species. *Plant Cell Environ.* **30**, 1176–1190. (doi:10.1111/j.1365-3040.2007.01690.x)
61 Berry, J. & Bjorkman, O. 1980 Photosynthetic response and adaptation to temperature in higher plants. *Annu. Rev. Plant Physiol.* **31**, 491–543. (doi:10.1146/annurev.pp.31.060180.002423)
62 Cunningham, S. C. & Read, J. 2003 Do temperate rainforest trees have a greater ability to acclimate to changing temperatures than tropical rainforest trees? *New Phytol.* **157**, 55–64. (doi:10.1046/j.1469-8137.2003.00652.x)
63 Kositsup, B., Montpied, P., Kasemsap, P., Thaler, P., Ameglio, T. & Dreyer, E. 2009 Photosynthetic capacity and temperature responses of photosynthesis of rubber trees (*Hevea brasiliensis* Müll. Arg.) acclimate to changes in ambient temperatures. *Trees Struct. Funct.* **23**, 357–365. (doi:10.1007/s00468-008-0284-x)
64 Deutsch, C. A., Tewksbury, J. J., Huey, R. B., Sheldon, K. S., Ghalambor, C. K., Haak, D. C. & Martin, P. R. 2008 Impacts of climate warming on terrestrial ectotherms across latitude. *Proc Natl Acad. Sci. USA* **105**, 6668–6672. (doi:10.1073/pnas.0709472105)
65 Le Page, Y., van der Werf, G. R., Morton, D. C. & Pereira, J. M. C. 2010 Modeling fire-driven deforestation potential in Amazonia under current and projected climate conditions. *J. Geophys. Res.* **115**, G03012. (doi:10.1029/2009JG001190)
66 Hasler, N. & Avissar, R. 2007 What controls evapotranspiration in the Amazon basin? *J. Hydrometeorol.* **8**, 380–395. (doi:10.1175/JHM587.1)
67 Mercado, L. M., Bellouin, N., Sitch, S., Boucher, O., Huntingford, C., Wild, M. & Cox, P. M. 2009 Impact of changes in diffuse radiation on the global land carbon sink. *Nature* **458**, 1014–1017. (doi:10.1038/nature07949)
68 Gullison, R. E. *et al.* 2007 Tropical forests and climate policy. *Science* **316**, 985–986. (doi:10.1126/science.1136163)
69 Ebeling, J. & Yasue, M. 2008 Generating carbon finance through avoided deforestation and its potential to create climatic, conservation and human development benefits. *Phil. Trans. R. Soc. B* **363**, 1917–1924. (doi:10.1098/rstb.2007.0029)
70 Aragao, L. & Shimabukuro, Y. E. 2010 The incidence of fire in Amazonian forests with implications for REDD. *Science* **328**, 1275–1278. (doi:10.1126/science.1186925)